Ultra-high resolution spectroscopy at 10 μm: Applications and new Trends

Ch. Chardonnet, A. Amy-Klein, V. Bernard, R.J. Butcher, P.E. Durand,
T. George, F. Guernet, H.W. Nicolaisen, O. Pfister, and Ch. J. Bordé,
Laboratoire de Physique des Lasers, URA n°282 du CNRS, Université Paris-Nord
Avenue J.-B. Clément, 93430 Villetaneuse

In saturation spectroscopy, the resolution which is usually limited by the finite transit time through the laser beam may be enhanced thanks to an optical selection of slow molecules. We present the conditions required for such a method and the experimental results which lead to a resolution of 80 Hz at 30 THz [1]. For such a resolution, the spectral characteristics of the laser are critical. For that reason, we have developed a new stabilization scheme and we present here the progress already achieved [2]. One fascinating application of ultra-high resolution would be to observe the parity violation in molecules induced by the weak interactions [3]. We show why parity-degenerate doublets, such as the E states of simple molecules, which were previously considered to detect such an effect are probably not the best candidates [4].

1. The optical selection of slow molecules

Up to now, there is no efficient scheme for laser cooling of molecules. Thus, the alternative is to use an optical selection of slow molecules whose enhanced contribution to the saturation signal has been predicted in 1976 [1]. The method has been proposed and demonstrated in Novosibirsk for methane at 3.39 μm with a large cell placed inside the laser cavity [1]. We have developed and adapted this method for the more general case of an external cell.

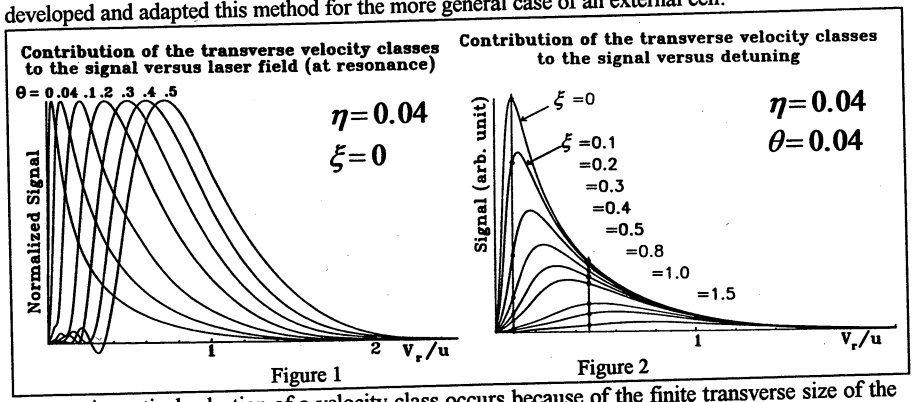

Figure 1

Figure 2

An optical selection of a velocity class occurs because of the finite transverse size of the laser beam, since the coherent interaction time between molecules and light and, thus, the saturation parameter depends on the transverse velocity of the molecules. For that reason, we introduce the transit width as a frequency unit : $\Gamma_{tr} = u/w_0$ where u is the most probable velocity and w_0 is the waist radius of the laser beam. Then, we define the three relevant parameters in units of transit width: $\eta = \frac{\gamma}{\Gamma_{tr}}$, the pressure broadening (the spontaneous emission can be neglected), $\theta = \frac{\Omega}{\Gamma_{tr}}$, the Rabi pulsation and $\xi = \frac{\Delta}{\Gamma_{tr}}$, the detuning of the laser frequency from the molecular resonance. No velocity selection can occur if the molecules are in the collisional regime ($\eta >> 1$) for which this interaction time is determined by the time between two collisions

mainly independent of the velocity. The velocity selection will occur effectively only when $\eta << 1$. Moreover, the slow molecules will give the main contribution to the signal only if $\theta << 1$. This is shown on Fig. 1 at resonance, where the maximum of the curves for which $\theta > \eta$, is obtained for the velocity class with the saturation parameter S~1. When $\theta << \eta$, then S<<1 for each velocity class. This is the weak-field regime for which the contribution is maximum for the velocity class, $v_r \sim \eta u$, i.e. the velocity is selected by the pressure. In order to keep some signal an experimental optimum is obtained for $\eta \sim \theta$. In that case, the three characteristic times associated to the selected velocity class are of the same order of magnitude: the mean time between two collisions, the transit time through the beam and the time required for the absorption of one photon. The inverse of this common time gives the expected resolution. However, Fig. 2 shows that the global line shape is strongly inhomogeneous since fast molecules give their main contribution to the signal in the wings of the resonance and are responsible for its broadening. This is due to the width of the resonance for each velocity class (illustrated by the intersection of the various curves of Fig.2 by vertical lines) which is proportional to the velocity when the molecules are in the free-flight regime ($v_r > \eta u$). Finally, one can take advantage of these differences between velocity classes by considering the derivative or the second derivative of the lineshape which magnifies the sharper signals (i.e. coming from the slow molecules). Experimentally, this is achieved by applying a modulation frequency smaller than the linewidth and by detecting the first or the second harmonic (Fig. 3). This method lead to the narrowest line recorded by our spectrometer. This improved its resolving power by one order of magnitude. The selected velocity class is about 5m/s while u=140m/s. The observation of a signal of a few 10^{-15} W has required heterodyne detection in order to get rid of the detector noise. As a nice illustration, we were able to resolve for the first time the hyperfine structure of a Q line in the ν_3 band of SF_6 with 7 hyperfine components in a range of 5.4 kHz (Fig.4).

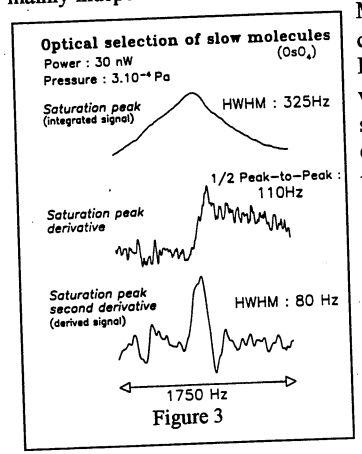

Figure 3

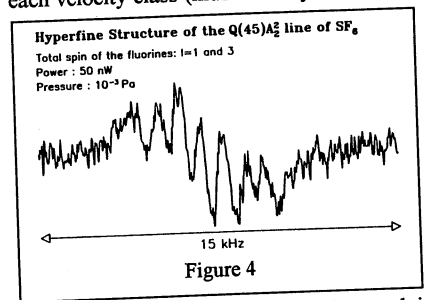

Figure 4

2. A new frequency stabilization scheme for CO_2 lasers

One important limitation of the previous experiments was the long term stability of the reference laser of the spectrometer. This laser was frequency-stabilized on a saturation line of a molecular gas placed in an external cell. It provided a spectral purity of about 10 Hz and a long-term stability of a few Hz/minute which limited seriously the accumulation time. Thus, we have started a new stabilization scheme for CO_2 lasers for which the short term and the long term stabilities are treated separately. For the short term stability, we will use a high finesse passive Fabry-Perot cavity and a theoretical linewidth of a few mHz is expected. Up to now, only the long term stabilization reference is operational; it is based on a saturation line with a cell placed in a Fabry-Perot cavity. This cavity increases the contrast of the saturation signal by a factor

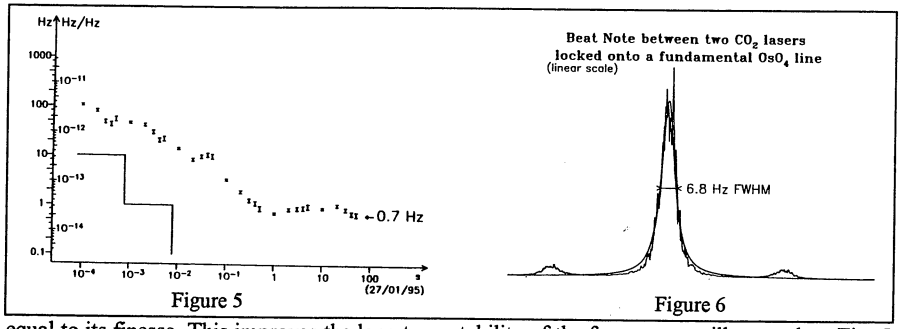

Figure 5

Figure 6

equal to its finesse. This improves the long term stability of the frequency as illustrated on Fig. 5 which shows the Allan variance of the beat note between two lasers locked independently. We can see the typical -1/2 slope of a white frequency noise which crosses at τ=1s the Flicker floor of 0.7 Hz, i.e. $\delta\nu/\nu=2.10^{-14}$. No drift was visible during 2000 s while the dispersion of the beat note frequency was only 3 Hz. Fig. 6 shows the beat note between two lasers fitted by a Lorentzian.

3. The role of Parity in molecular spectra

The observation of parity violation in molecular spectra could be a very nice application of ultra-high resolution spectroscopy and, as a matter of fact, the state-of-the-art of ultra-stable lasers seems to be compatible now with the order of magnitude of the estimated effect. Then, one key point is the choice of the molecule. Two routes have been suggested: the first one is to compare the energies of right- and left-handed chiral molecules; the second one is to study E states of simple molecules which are known to be parity-degenerate. A lifting of the degeneracy may be the signature of weak interactions. We will show that, actually, hyperfine interactions will very likely mask this effect.

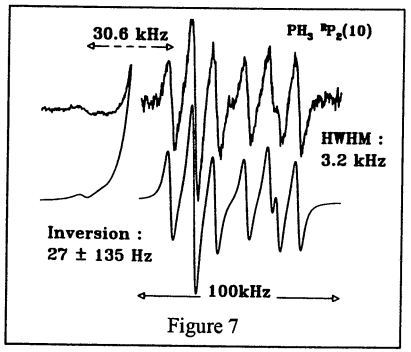

Figure 7

We have resolved the hyperfine structure of the $^RP_2(10)$ line in the ν_4 band of PH_3 (Fig. 7). Although this molecule has the same geometry as ammonia, the inversion splitting, in that case, is very small and expected to be less than one Hz. We introduce: I_P=1/2, the spin of the phosphorus, I_H=1/2 or 3/2, the total spin of the hydrogens; J, the orbital angular momentum; K, its projection on the molecular axis and τ, the total parity. For K=2, the rovibrational level is parity-degenerate and because of the Pauli principle, I_H is 1/2. Finally, we expect to observe four main hyperfine lines twice degenerate in parity. Fig. 7 shows a spectrum with 8 main components (with small crossovers on the left-hand side) almost fully resolved. We explain now why the hyperfine lines of opposite parity may have different energies even if inversion is negligible. Let us look in more detail how a total wavefunction is built. It is a tensorial product of orbital and nuclear spin wavefunctions: $\psi_{tot.} = \psi_{orb.} \otimes \psi_{n.s.}$. Any wavefunction can be classified according to the 3 representations of the molecular point group (i.e. C_{3V}). A_1 and A_2 are, respectively, the totally symmetric and antisymmetric representations, E is a representation of dimension 2. Since the hydrogens are fermions, the symmetry of $\psi_{tot.}$ must be

A_2. The orbital wavefunctions, $\psi_{orb.}$ with $|K|$=2 form two E representations $\{ |K,\tau>, |-K,\tau> \}$, one per parity. Without inversion, they form four orbital degenerate states. In order to build an A_2 total wavefunction, we need to combine the orbital part with nuclear wavefunctions belonging also to a E representation. A typical example would be:

$$\{\frac{1}{\sqrt{3}}(|-++>+\varepsilon|+-+>+\varepsilon^2|++->);\frac{1}{\sqrt{3}}(|++->+\varepsilon|-++>+\varepsilon^2|+-+>)\}$$

$\varepsilon = \exp\left(\frac{2i\pi}{3}\right)$ and we have ignored the phosphorus spin. Finally, in order to build the total wavefunction of a given hyperfine state which may be characterized by the values of $\mathbf{F_1=J+I_P}$ and $\mathbf{F=F_1+I_H}$, one starts from 4x2 states before applying the Pauli principle. These are represented on Fig. 8. First, inversion may lift the degeneracy in parity. Second, the representation ExE is reducible in A_1+A_2+E and hyperfine interactions may lift the degeneracy. Of course, this hyperfine structure is exactly the same for (+) and (-) levels. However, the key point is that if we change only the parity character of a total wavefunction, the symmetry characters, A_1 and A_2, are exchanged. This can be checked on a typical total wavefunction:

$$\frac{1}{\sqrt{6}}\Big[\ (|K,\tau>\pm(-1)^\tau|-K,\tau>)|-++>+\varepsilon(|K,\tau>\pm(-1)^\tau\varepsilon|-K,\tau>)|+-+>$$
$$+\varepsilon^2(|K,\tau>\pm(-1)^\tau\varepsilon^2|-K,\tau>)|++->\ \Big]$$

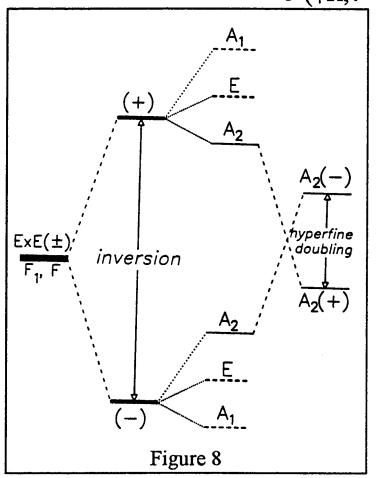

Figure 8

where the sign + (resp. -) corresponds to a A_1 (resp. A_2) state and where $(-1)^\tau$ is ±1 for τ=(±). Finally, for a molecule with no inversion, the two hyperfine structures are superimposed and the Pauli principle restricts the existing states to the A_2 states of opposite parity which do not have the same rovibrational structure.

This is, actually, a general rule: if the molecular point group contains an odd operation, symmetric and antisymmetric characters are exchanged with the change of parity alone. For that reason, two existing states with different parities differ also by their rovibrational structure and, thus, may have different energies. In the case of PH_3, a tensorial hyperfine term is responsible for the lifting of degeneracy of this isolated rovibrational level. In the case of SiF_4, for which the E states have a total spin of the fluorine's equal to zero, we have also observed a lifting of degeneracy due to tensorial hyperfine couplings with neighbouring rovibrational levels. However, molecules with no identical nuclei can have identical states except for parity, since the Pauli principle does not apply. Chiral molecules may be of this kind and, for such degenerate states, weak interactions lift the degeneracy at the first order, if inversion is negligible.

4. References

1. Ch. Chardonnet, F. Guernet, G. Charton, Ch.J. Bordé, *Appl. Phys.* **B59** (1994) 333 and ref. therein.
2. V. Bernard, P.E. Durand, T. George, H.W. Nicolaisen, A. Amy-Klein, Ch. Chardonnet, submitted to *IEEE J. Quant. Electron.*
3. V.S. Letokhov, *Phys. Lett.* **A53** (1975) 275.
4. R.J. Butcher, Ch. Chardonnet, Ch.J. Bordé, *Phys. Rev. Lett.* (1993) 2698.